Carbohydrate Polymers 80 (2010) 65–70

Contents lists available at ScienceDirect

Carbohydrate Polymers

journal homepage: www.elsevier.com/locate/carbpol

Adsorption of chitosan on spin-coated cellulose films

A.L. Da Róz [a,*], F.L. Leite [c], L.V. Pereiro [a], P.A.P. Nascente [b], V. Zucolotto [a], O.N. Oliveira Jr. [a], A.J.F. Carvalho [c]

[a] Instituto de Física de São Carlos, Universidade de São Paulo (USP), São Carlos, Brazil
[b] Universidade Federal de São Carlos, Campus São Carlos, Brazil
[c] Universidade Federal de São Carlos, Campus de Sorocaba, Brazil

ARTICLE INFO

Article history:
Received 30 September 2009
Received in revised form 20 October 2009
Accepted 28 October 2009
Available online 5 November 2009

Keywords:
Cellulose
Chitosan
AFM
XPS
Thin films
Spin-coating

ABSTRACT

This paper reports on the adsorption of an ultrathin chitosan layer on spin-coated films of cellulose, where efficient attachment was induced by oxidizing cellulose which provided anionic sites for electrostatic interaction with the positively charged chitosan. Both the cellulose oxidation and the chitosan adsorption were confirmed with Fourier transform infrared spectroscopy (FTIR) and X-ray photoelectron spectroscopy (XPS) measurements. The molecular-level interaction between chitosan and cellulose involved the N—H groups, as inferred from the disappearance caused by chitosan adsorption of the amide band at 1667 cm^{-1} in the FTIR spectrum of cellulose. The XPS data confirmed a significant increase in the atomic concentration of nitrogen groups, from 2.16% to 4.73% when chitosan was adsorbed on the oxidized cellulose film, which also led to rougher films as illustrated by atomic force microscopy images. One may now envisage applications in which the bactericide action of chitosan is combined with the biocompatibility of cellulose.

1. Introduction

The increasing use of cellulose in the pharmaceutical and papermaking industries has demanded a refined understanding of its physicochemical properties, processability and molecular-level interactions (Kontturi, Thune, & Niemantsverdriet, 2003). Because cellulose is insoluble in most organic and inorganic solvents, a detailed investigation of interactions with other materials is not straightforward. This limitation can be overcome by processing cellulose in the form of ultrathin films (Eriksson, Notley, & Wågberg, 2007; Falt, Wagberg, Vesterlind, & Larsson, 2004; Gunnars, Wågberg, & Stuart, 2002; Holmberg et al., 1997; Kondo, Kasai, & Brown, 2004; Kontturi, Tammelin, & Osterberg, 2006; Kontturi et al., 2003; Notley, Eriksson, Wågberg, Beck, & Gray, 2006; Radtchenko, Papastavrou, & Borkovec, 2005; Sczech & Riegler, 2006; Yokota, Kitaoka, & Wariishi, 2007). Thin films were first produced with cellulose derivatives, *e.g.* trimethylsiloxane cellulose (TMSC) (Amim, Kosaka, & Petri, 2008; Holmberg et al., 1997; Kontturi et al., 2003; Radtchenko et al., 2005; Tammelin, Saarinen, Sterberg, & Laine, 2006), whose surface properties differed from those of cellulose *in natura*. Another widely used strategy is the fabrication of cellulose films via its solubilization in organic solvents such as *N*-methylmorpholine-*N*-oxide (NMNO) (Eriksson et al., 2005, 2007; Freudenberg et al., 2005; Gunnars et al., 2002; Notley et al., 2006; Yokota et al., 2007), dimethylthexylsilyl chloride (TDMSCl) (Kadla, Asfour, & Bar-Nir, 2007), aqueous NaOH/thiourea solutions (Yan, Wang, & Chen, 2008) and lithium chloride (LiCl) in dimethylacetamide (DMAc) (Eriksson et al., 2005, 2007; Kondo et al., 2004; Notley et al., 2006; Radtchenko et al., 2005; Sczech & Riegler, 2006; Wang, Chen, & Kim, 2007).

The possible control of molecular architectures and film properties afforded by methods such as the layer-by-layer (LbL) technique (Decher, 1997; Leite et al., 2005) can be exploited in optimizing the properties of cellulose. In this study, we covered spin-coated cellulose films with a one-layer chitosan film adsorbed via electrostatic interactions. The motivation for employing chitosan, a nontoxic and antimicrobial copolymer consisting of β-(1,4)-2-acetamido-2-deoxy-D-glucose and β-(1,4)-2-amino-2-deoxy-D-glucose units, lies in the possible antimicrobial activity (Jeon, Park, & Kim, 2001; No, Park, Lee, & Meyers, 2002). Existing methods to incorporate chitosan into cellulose are based on the treatment of cellulose fibers with chitosan, where the latter is anchored physically to the fibers. Here, we improved chitosan adsorption by oxidizing cellulose, which then had effective anchoring sites for chitosan. The investigation of the anchoring process in a thin film instead of in naturally occurring fibers showed to be more convenient and an interesting tool to study cellulose interactions with other biomolecules.

2. Experimental

2.1. Materials

Glass slides coated with a gold layer were used as substrates. Microcrystalline cellulose (type PH-101, Avicel® – FMC – Belgium,

* Corresponding author.
E-mail address: alessandra.roz@gmail.com (A.L. Da Róz).

0144-8617/$ - see front matter © 2009 Elsevier Ltd. All rights reserved.
doi:10.1016/j.carbpol.2009.10.062

with an average particle size of 50 μm) was used as raw material. Dimethylacetamide (DMAc – Vetec – Brazil) was distilled from CaH_2 (Aldrich) and kept over activated 4 Å molecular sieves. Lithium chloride (LiCl – Mallinckrodt – USA) was dried at 200 °C for 3 h and kept in a desiccator. Chitosan from shrimp was purchased from Galena Chemistry, Brazil (120 Cps of viscosity and 85% deacetylation). Phosphoric acid (Synth Brazil), nitric acid (Quimis – Brazil) and sodium nitrite (Hoecht) were used as oxidant agents. Ninidryn (Mallinckrodt – USA), sodium acetate (Synth – Brazil) and methylene blue dye were used as received.

2.2. Cellulose dissolution

Cellulose powder (Avicel) was dissolved in a solution of LiCl in DMAc employing a procedure adapted from Ramos, Assaf, El Seoud, and Frollini (2005). Briefly, 2 g of dry cellulose and 5 g of LiCl were kept under constant stirring, and heated from room temperature to 110 °C at a rate of 3 °C/min to ensure water removal. After 1 h, 100 mL of DMAc were slowly added, and the system was heated from 110 to 160 °C at 4 °C/min under vigorous stirring. After 1 h, the system was slowly cooled to 36 °C at 1 °C/min, maintained by stirring for 24 h.

2.3. Cellulose films preparation

Cellulose films were produced by the spin-coating technique. The glass substrate was covered with the cellulose solutions and spun at spin speeds of 1500 and 2500 rpm for 12 min. The slide was dried at 90 °C under vacuum. After dried, the film was thoroughly washed in deionized water. Finally, the slides were dried under a nitrogen flow and stored at 25 °C.

2.4. Oxidation of the thin cellulose film surface

The oxidation process of cellulose films was performed using a solution of 0.0355 g of sodium nitrite in a mixture of 5 mL of phosphoric and nitric acids (1/1 v/v) in deionized water (¼ of acid solution volume). The cellulose films were immediately immersed in the solution for 15 s at 25 °C, followed by film washing in deionized water and drying under a nitrogen flow.

2.5. Adsorption of chitosan

The cellulose samples were immersed in the chitosan solution (1 wt.%) in acetic acid (1 wt.%) (∼pH 2.7) for 1 min, followed by washing in deionized water and drying at 115 °C, in a procedure similar to those employed in the LbL technique (Leite et al., 2005).

2.6. Characterization

The oxidation of cellulose films and its interaction with chitosan were monitored by measuring the infrared spectra with a FTIR spectrometer BOMEM MB-102. Cellulose films were analyzed in the reflection mode, whereas cellulose powder was investigated using the transmission mode with KBr pellets (100:1). The oxidation of the cellulose films was also monitored using UV–vis absorption spectra obtained with a HITACHI (U-2001) spectrophotometer.

X-ray diffraction patterns were acquired with a Rigaku X-ray diffractometer with Cu K ($\lambda = 1.542$ Å) radiation, submitted to 50 kV/100 mA, with scan speed of 2°/min (normal), grazing incidence angle of 2° and exposed to radiation from 3° to 40° (2θ). The crystallinity index *CrI* was estimated by employing the definition of Duchemin, Newman, and Staiger (2007), as $CrI = \left(\frac{Hc}{Ha} + Hc\right) \times 100$, where *Hc* is the height of the peak typically located in the range $2\theta = 21$–$22°$ and *Ha* is the height measured at $2\theta = 15°$, which is related to the amorphous cellulose.

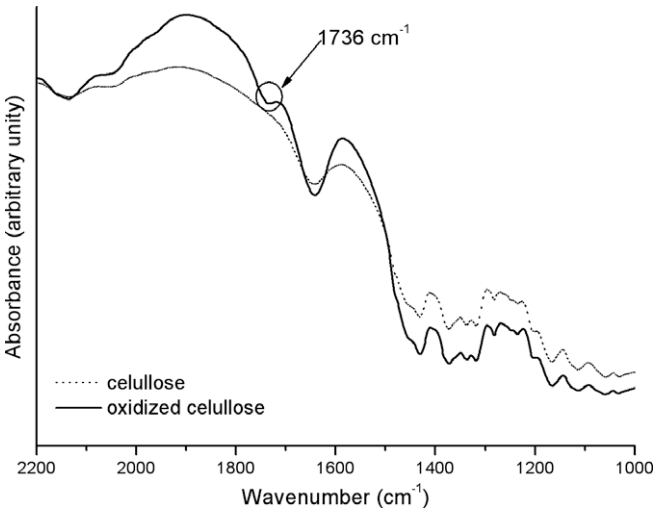

Fig. 1. FTIR spectra for the unmodified and oxidized cellulose.

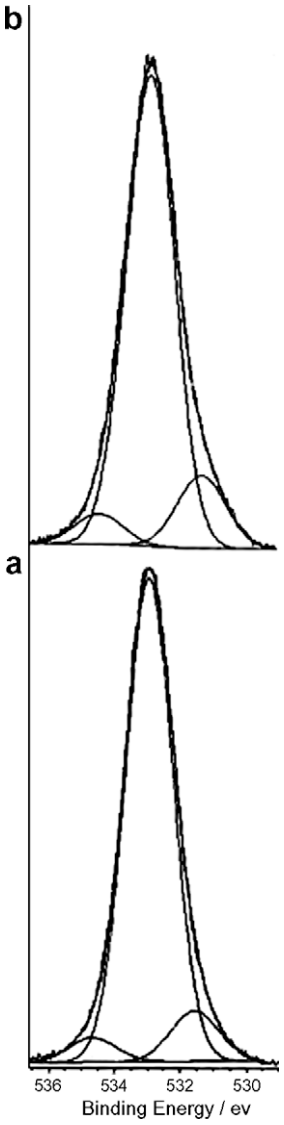

Fig. 2. High resolution XPS spectra of the O1s peak for cellulose films: (a) non-oxidized and (b) oxidized.

X-ray photoelectron spectroscopy (XPS) analysis was performed with a Kratos XSAM HS spectrometer, using monochromatized Mg Kα radiation. The spectrometer was operated at 49 W, 7 kV, and 7 mA, and the photon energy was 1253.6 eV. A pass energy of 80 eV was used for high-resolution scans in a valence band analysis. The spot size was 15 × 15 × 1 mm. The binding energies for all spectra were determined with respect to the C1s reference signal (C—H or C—C bands) at 285.0 eV. The Shirley background and Gaussian/Lorentzian functions were used for fitting the peaks.

The surface features and roughness of spin-coated cellulose films were evaluated with atomic force microscopy (AFM). The AFM images were taken with a Nanoscope IIIa Multimode microscope (Digital Instruments Inc.). Samples were scanned with a silicon cantilever with spring constant of 20 N/m and tip radius of 10 nm (nominal values). All measurements were performed in the tapping mode® under ambient conditions. The AFM images were analyzed using WSxM 4.0 software (Nanotec Electronica S.L.) (Horcas et al., 2007).

3. Results and discussion

3.1. Formation and characterization of cellulose films

Fig. 1 shows the FTIR spectra of the cellulose spin-coated films, with typical bands for cellulose at 3400–3450 cm^{-1} (hydroxyl groups), 2880–2900 cm^{-1} (C—H stretching) and 1150–1085 cm^{-1} (ether bonding). No peak assigned to residual DMAc was observed in the cellulose films, which indicates that the washing procedure was efficient in removing the solvent. In many cases, anchoring polymers are used to promote the adhesion of cellulose onto the substrates (Falt et al., 2004; Gunnars et al., 2002; Notley et al., 2006), but this was not necessary here, since cellulose films easily attached to the glass surface. The presence of cellulose was confirmed with the XPS data, shown in Fig. 2a and Table 1. The observed oxygen and C—O contribution at 286.7 eV, leading to C 59% and O 49%, are similar to the theoretical values for the $C_6H_{10}O_5$ units (Burrell, Butts, Derr, Genovese, & Perry, 2004). Only a small amount of nitrogen was detected, possibly arising from residual solvent.

The X-ray diffractogram for the raw microcrystalline cellulose powder (Avicel) displayed peaks at $2\theta = 10.37°$, 19.96°, 21.90° and 35.40°, as shown in Fig. 3a, which are typical of native crystalline cellulose I (Isogai, Usuda, Kat, Uryu, & Atalla, 1989). In contrast, Fig. 3b shows that the spin-coated cellulose film obtained from solution in LiCl/DMAc exhibited peaks at $2\theta = 11.80°$ and 21.00° typical of cellulose III and analogous to the structure of regenerated cellulose (Isogai et al., 1989). The transformation of cellulose I into cellulose III upon processing cellulose in the form of thin films may be attributed to the treatment with liquid ammonia or organic amines (Isogai et al., 1989; Wada, Nishiyama, & Langan, 2006). The broad peak at $2\theta = 21.0°$ with a width of approximately 9°, suggests that the two diffraction peaks from cellulose I combine into a single broad peak in cellulose III (Duchemin et al., 2007). The peak at $2\theta = 35.3°$ from cellulose I (Fig. 3a) was absent in the diffractogram of cellulose III, which suggests disorder, consistent with a semicrystalline matrix (Duchemin et al., 2007). Indeed, the diffraction peaks for cellulose III in the films were broader, pointing to a low crystallinity, with the crystallinity index, *CrI*, decreasing from 83% for cellulose I to 67% for the film (cellulose III), in agreement with Duchemin et al. (2007).

Table 1
XPS ratio and semi-quantified atomic concentration for various samples.

Sample	Concentration (atomic%)			Ratio	
	C	O	N	$O_2/(C_2 + C_3)$	C_3/C_2
Cellulose thin film	58.79	38.84	1.22	0.78	0.25
Cellulose thin film coated with chitosan	65.37	30.54	2.16	0.67	0.28
Oxidized cellulose thin film	54.91	40.60	1.24	0.90	0.26
Oxidized cellulose thin film coated with chitosan	44.81	44.43	4.73	0.93	0.29

Fig. 4 shows the AFM images of gold substrates and cellulose films spin-coated at 2500 rpm. The surface of gold in Fig 4a exhibited a flat, smooth topography with root mean square (RMS) roughness of ≈2.6 nm. For the cellulose film in Fig. 4b, the roughness was ca. 13 nm owing to irregularities with a dense distribution of fibers. This roughness differs from those of cellulose films in the literature (Notley et al., 2006; Radtchenko et al., 2005; Szczech & Riegler, 2006), which were less rough. The differences may be attributed to changes in the deposition method, solution preparation, and film thickness.

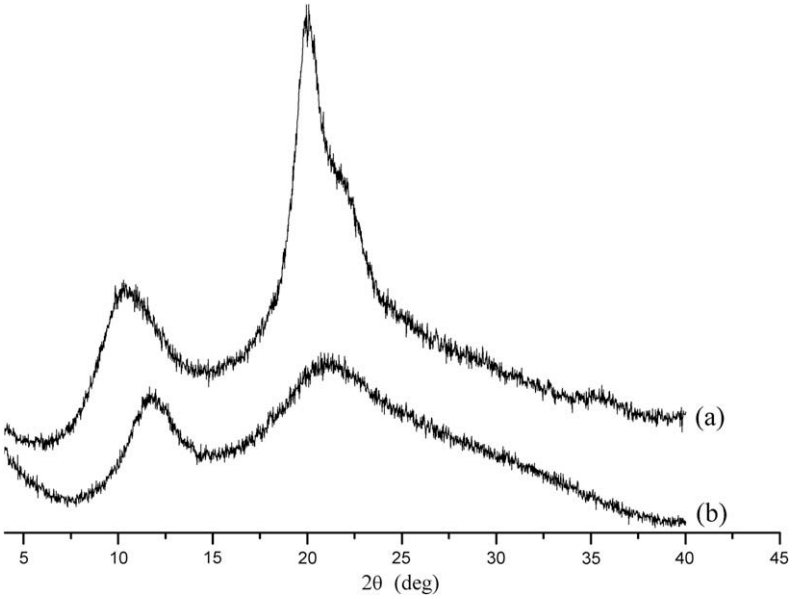

Fig. 3. X-ray diffraction pattern of (a) native cellulose and (b) cellulose thin film.

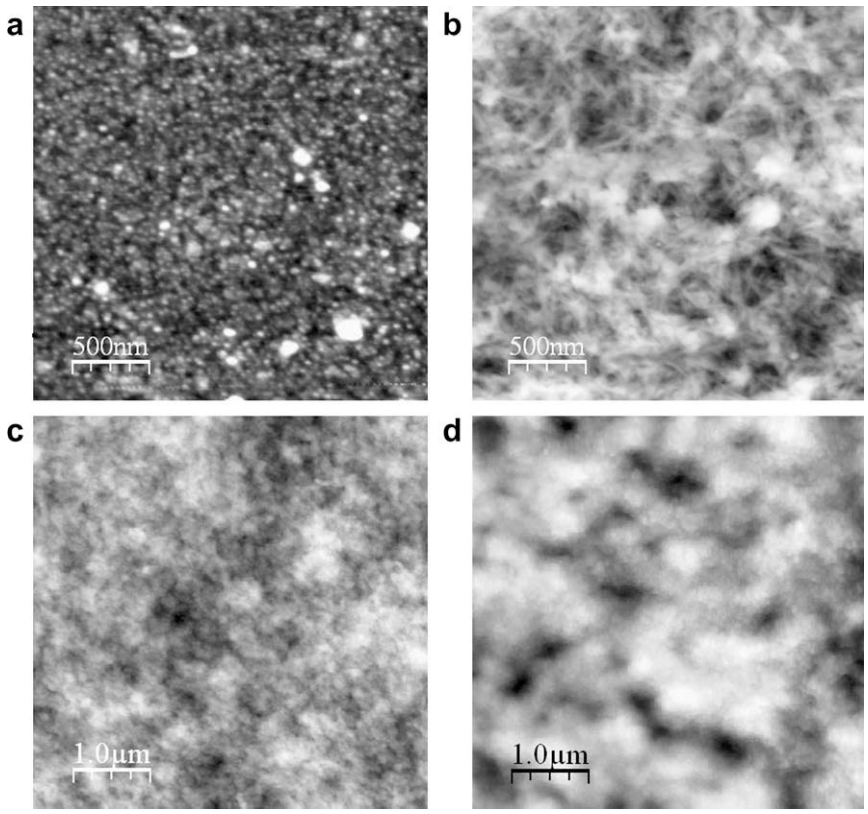

Fig. 4. AFM images of (a) gold pattern (RMS = 2.6 nm, 2.5 × 2.5 μm), (b) cellulose films (RMS = 13.0 nm, 2.5 × 2.5 μm), (c) oxidized cellulose film (RMS = 11 nm, 5 × 5 μm) and (d) oxidized cellulose film covered with chitosan (RMS = 33 nm, 5 × 5 μm).

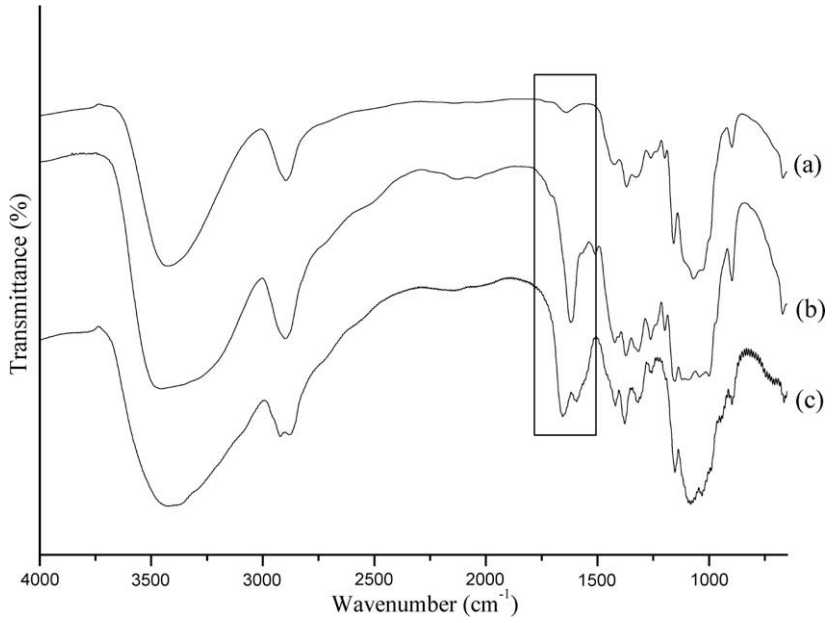

Fig. 5. FTIR spectra showing anchoring of chitosan on the cellulose thin film: (a) cellulose thin film, (b) cellulose thin film coated with chitosan and (c) chitosan thin film.

3.2. Oxidation of cellulose films

The oxidation of cellulose films was carried out to increase adhesion between cellulose and chitosan. Oxidation can produce carboxylic acid groups that may interact electrostatically with chitosan forming ion pairs. To verify whether oxidation was successful, UV–vis analyses were carried out using methylene blue as a colorant. The idea behind this approach is that a stronger attachment of the cationic dye is achieved in the oxidized films. Table 2 shows the absorbance at 660 nm for the dye, and non-modified and oxidized cellulose films. Oxidized cellulose exhibits a stronger attachment to the dye (2×) than for non-modified cellulose, which points to the formation of anionic sites in the oxidized films. This has important implications for the adsorption of chitosan through electrostatic interactions, as will be discussed later on.

Table 2
Absorbance values at 660 nm for the various samples investigated.

Sample	Absorbance at 660 nm
Methylene blue	0.048
Cellulose thin film	0.038
Cellulose thin film + methylene blue	0.046
Oxidized cellulose thin film + methylene blue	0.110

We also obtained high-resolution O1s XPS spectra for cellulose and oxidized cellulose. Fig. 2 shows the spectra resolved into three Gaussian/Lorentzian components for non-oxidized and oxidized cellulose films, the most intense of which was centered at 533.0 eV, attributed to electrons from oxygen atoms that are bonded to hydrogen atoms (OH) (Beamson & Briggs, 1992; Danielache et al., 2005; Matienzo & Winnacker, 2002). Another component located at 534.5 eV is assigned to electrons from oxygen atoms bonded to one carbon atom (—O—) (Shen, Anand, & Levicky, 2004), while the third component at 531.4 eV is assigned to carbonyl groups C=O (Beamson & Briggs, 1992) resulting from oxidation. The presence of surface oxidation products and contaminants also contributed to some extent to the O1s spectrum, with slight excess of oxygen in most of the complexes (Table 1). Cellulose oxidation was confirmed by the increase in the relative amount of carbonyl groups from 9% for cellulose to 13% for oxidized cellulose. In addition, the oxidation (O incorporation) led to an increase in the O/C ratio, from 0.78 to 0.90. The theoretical O/C ratio for pure cellulose is 0.83, which should not be altered upon conversion of primary alcohol into aldehyde. If the oxidation proceeds with the formation of a carboxyl group, the O/C ratio should change to 1, as shown in Table 1 (DiFlavio et al., 2007). In summary, the XPS results confirmed the increase in the number of anionic sites in the cellulose films upon oxidation.

Consistent with the XPS and UV–vis data, the FTIR spectrum for an oxidized cellulose film in Fig. 1 displayed a shoulder at 1736 cm^{-1} assigned to carbonyl groups (El-Hendawy, 2006; Lojewska, Miskowiec, Lojewski, & Proniewicz, 2005), which should be only due to the difference between the spectra of oxidized and non-oxidized cellulose (Aimin, Hongwei, Gang, Guohui, & Wenzhi, 2005). The oxidation process induced a change in surface morphology, as indicated in the AFM images of Fig. 4b and c. A possible explanation is that the acidic treatment induces deterioration of the film surface, resulting in removal of material.

3.3. Adsorption of chitosan on cellulose

Fig. 5 shows the FTIR spectra for films of cellulose, chitosan and cellulose coated with a layer of chitosan adsorbed via electrostatic interactions, as in the LbL technique (Decher, 1997; Leite et al., 2005). The FTIR spectrum for the neat chitosan film displays bands at 3400–3450 cm^{-1} (hydroxyl groups stretching vibration), 3300 and 3200 cm^{-1} (symmetric and asymmetric NH stretching), 2874–2922 cm^{-1} (C—H stretching), 1667 cm^{-1} (C=O, amide I), 1591 cm^{-1} (N—H deformation), 1380 cm^{-1} (CH_3 deformation), 1309 cm^{-1} (C—N stretching, amide III), 1079 cm^{-1} (amine C—N stretching vibration) and 1150–1085 cm^{-1} (ether bonding) (Rosca, Popa, Lisa, & Chitanu, 2005; Silverstein, Bassler, & Morril, 1994). Differences between chitosan and cellulose spectra may be observed at 1667 and 1591 cm^{-1} bands, attributed to C=O (amide I) and N—H groups from chitosan, respectively. For the cellulose film coated with a layer of chitosan, these two bands are combined and shifted to 1617 cm^{-1}. The disappearance of the band from amide I at 1667 cm^{-1} indicates that N—H groups from chitosan interact with carbonyl groups, thus confirming the molecular interaction between cellulose and chitosan (Lima, Lazarin, & Airoldi, 2005). This is a typical feature of films produced with the LbL method owing to the intimate contact between adjacent layers (Zucolotto et al., 2003).

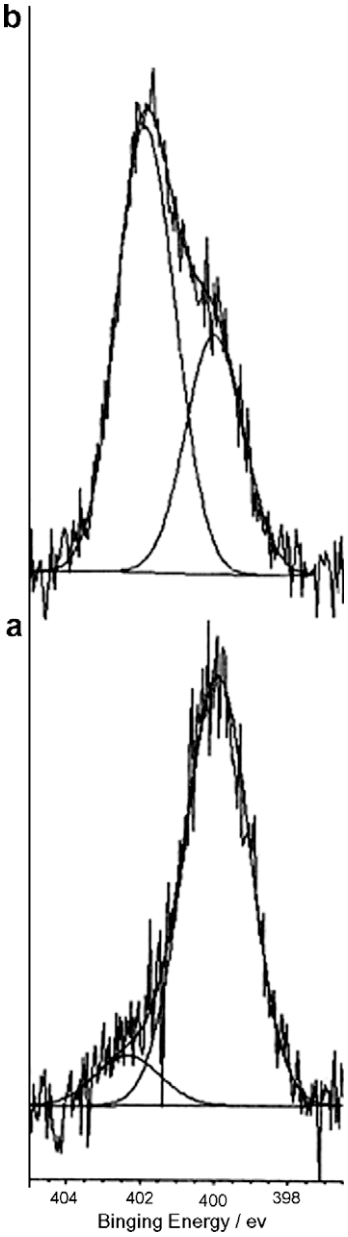

Fig. 6. High resolution XPS spectra of the N1s peak of (a) cellulose and (b) oxidized cellulose, both with adsorbed chitosan.

The XPS data were also useful to study the chitosan adsorption. The high-resolution N1s spectra for films of cellulose and oxidized cellulose, both coated with a chitosan layer, are shown in Fig. 6. The most intense component centered at 400.0 eV is due to electrons from nitrogen atoms that are bonded to carbon atoms (N—C) or non-protonated amine groups (Matienzo & Winnacker, 2002). A second peak at 401.9–402.4 eV is attributed to the oxidized nitrogen or to a protonated nitrogen (Dambies, Guimon, Yiacoumi, & Guibal, 2001; Matienzo & Winnacker, 2002). The anchoring of very little chitosan is consistent with the small increase in the atomic concentration of nitrogen groups, from 1.22 for cellulose to 1.24% for the same films after chitosan adsorption, as indicated in Table 1. This shows that the untreated cellulose film hardly anchors chitosan. A similar analysis showed the increase in nitrogen concentration after oxidation of the cellulose film, from 2.16% to 4.73% (Table 1), a further evidence of the efficiency of

the oxidation reaction in increasing the anchoring sites and consequently chitosan adsorption.

The adsorption of chitosan on the spin-coated cellulose films led to changes in surface morphology, as indicated in the tapping mode AFM images of Fig. 4. Upon adsorption of chitosan the surface texture became irregular, with a much larger roughness, i.e. >30 nm in Fig. 4d in comparison to 11 nm for the oxidized cellulose with no chitosan adsorption.

In summary, the results from AFM, XPS and FTIR demonstrated a high compatibility between chitosan and oxidized cellulose, probably due to interchain bonding, as reported for cellulose acetate/chitosan films (Lima et al., 2005).

4. Conclusions

Spin-coated cellulose films could be obtained from a cellulose solution in DMAc/LiCl, in which the crystalline structure was typical of cellulose III, i.e. with low crystallinity. The direct oxidation of hydroxyl groups in such films, confirmed with FTIR spectroscopy and XPS, provided anchoring sites for the adsorption of chitosan via electrostatic interactions. The molecular-level interaction between positively charged groups from chitosan and negatively charged groups from the cellulose film surface was inferred from the disappearance of the amide I and/or amide II band at 1667 cm^{-1} in the FTIR spectrum of cellulose upon chitosan adsorption. This indicated that N—H groups were involved in such molecular-level interactions, which were ultimately responsible for the enhanced adsorption of chitosan on the oxidized cellulose film. The adsorption of a chitosan layer on the cellulose film also induced morphological changes, with increased film roughness. The successful adsorption of chitosan onto cellulose opens the way for a number of applications, where the properties of biocompatibility and antimicrobian or bactericide activities may be combined.

Acknowledgments

This work was supported by FAPESP, CNPq and CAPES (Brazil).

References

Aimin, T., Hongwei, Z., Gang, C., Guohui, X., & Wenzhi, L. (2005). Influence of ultrasound treatment on accessibility and regioselective oxidation reactivity of cellulose. *Ultrasonics Sonochemistry, 12*, 467–472.

Amim, J., Jr., Kosaka, P. M., & Petri, D. F. S. (2008). Characteristics of thin cellulose ester films spin-coated from acetone and ethyl acetate solutions. *Cellulose, 15*(4), 527–535.

Beamson, G., & Briggs, D. (1992). Lineshapes. In *High resolution XPS of organic polymers. The scienta ESCA 300 database* (pp. 33–36). Chichester: John Wiley & Sons Ltd.

Burrell, M. C., Butts, M. D., Derr, D., Genovese, S., & Perry, R. J. (2004). Angle-dependent XPS study of functional group orientation for aminosolicone polymers adsorbed onto cellulose surfaces. *Applied Surface Science, 227*, 1–6.

Dambies, L., Guimon, C., Yiacoumi, S., & Guibal, E. (2001). Characterization of metal ion interactions with chitosan by X-ray photoelectron spectroscopy. *Colloids and Surfaces A: Physicochemical and Engineering Aspects, 177*, 203–214.

Danielache, S., Mizuno, M., Shimada, S., Endo, K., Ida, T., Takaoka, K., et al. (2005). Analysis of 13C NMR chemical shielding and XPS for cellulose and chitosan by DFT calculations using the model molecules. *Polymer Journal, 37*(1), 21–29.

Decher, G. (1997). Fuzzy nanoassemblies: Toward layered polymeric multicomposites. *Science, 277*, 1232–1237.

DiFlavio, J.-L., Pelton, R., Leduc, M., Champ, S., Essig, M., & Frechen, T. (2007). The role of mild TEMPO–NaBr–NaClO oxidation on the wet adhesion of regenerated cellulose membranes with polyvinylamine. *Cellulose, 14*(3), 257–268.

Duchemin, B. J.-C. Z., Newman, R. H., & Staiger, M. P. (2007). Phase transformations in microcrystalline cellulose due to partial dissolution. *Cellulose, 14*, 311–320.

El-Hendawy, A.-N. A. (2006). Variation in the FTIR spectra of a biomass under impregnation, carbonization and oxidation conditions. *Journal of Analytical and Applied Pyrolysis, 75*, 159–166.

Eriksson, J., Malmsten, M., Tiberg, F., Callisen, T. H., Damhus, T., & Johansen, K. S. (2005). Enzymatic degradation of model cellulose films. *Journal of Colloid and Interface Science, 284*, 99–106.

Eriksson, M., Notley, S. M., & Wågberg, L. (2007). Cellulose thin films: Degree of cellulose ordering and its influence on adhesion. *Biomacromolecules, 8*, 912–919.

Falt, S., Wagberg, L., Vesterlind, E.-L., & Larsson, P. T. (2004). Model films of cellulose II–improved preparation method and characterization of the cellulose film. *Cellulose, 11*, 151–162.

Freudenberg, U., Zschoche, S., Simon, F., Janke, A., Schmidt, K., Behrens, S. H., et al. (2005). Covalent immobilization of cellulose layers onto maleic anhydride copolymer thin films. *Biomacromolecules, 6*, 1628–1634.

Gunnars, S., Wågberg, L., & Stuart, M. A. C. (2002). Model films of cellulose: I. Method development and initial results. *Cellulose, 9*, 239–249.

Holmberg, M., Berg, J., Stemme, S., Dberg, L. O., Rasmusson, J., & Claesson, P. (1997). Surface force studies of Langmuir–Blodgett cellulose films. *Journal of Colloid and Interface Science, 186*, 369–381.

Horcas, I., Fernández, R., Gómez-Rodriguez, J. M., Colchero, J., Gómez-Herrero, J., & Baro, A. M. (2007). WSXM: A software for scanning probe microscopy and a tool for nanotechnology. *Review of Scientific Instruments, 78*, 013705.

Isogai, A., Usuda, M., Kat, T., Uryu, T., & Atalla, R. H. (1989). Solid-state CP/MAS 13C NMR study of cellulose polymorphs. *Macromolecules, 22*, 3168–3172.

Jeon, Y. J., Park, P. J., & Kim, S. K. (2001). Antimicrobial effect of chitooligosaccharides produced by bioreactor. *Carbohydrate Polymers, 44*(1), 71–76.

Kadla, J. F., Asfour, F. H., & Bar-Nir, B. (2007). Micropatterned thin film honeycomb materials from regiospecifically modified cellulose. *Biomacromolecules, 8*(1), 161–165.

Kondo, T., Kasai, W., & Brown, R. M. Jr., (2004). Formation of nematic ordered cellulose and chitin. *Cellulose, 11*, 463–474.

Kontturi, E., Tammelin, T., & Osterberg, M. (2006). Cellulose – model films and the fundamental approach. *Chemical Society Reviews, 35*(12), 1287–1304.

Kontturi, E., Thune, P. C., & Niemantsverdriet, J. W. (2003). Novel method for preparing cellulose model surfaces by spin coating. *Polymer, 44*, 3621–3625.

Leite, F. L., Paterno, L. G., Borato, C. E., Herrmann, P. S. P., Oliveira, O. N., & Mattoso, L. H. C. (2005). Study on the adsorption of poly(o-ethoxyaniline) nanostructured films using atomic force microscopy. *Polymer, 46*(26), 12503–12510.

Lima, I. S., Lazarin, A. M., & Airoldi, C. (2005). Favorable chitosan/cellulose film combinations for copper removal from aqueous solutions. *International Journal of Biological Macromolecules, 36*, 79–83.

Lojewska, J., Miskowiec, P., Lojewski, T., & Proniewicz, L. M. (2005). Cellulose oxidative and hydrolytic degradation: In situ FTIR approach. *Polymer Degradation and Stability, 88*, 512–520.

Matienzo, L. J., & Winnacker, S. K. (2002). Dry processes for surface modification of a biopolymer: chitosan. *Macromolecular Materials and Engineering, 287*, 871–880.

No, H. K., Park, N. Y., Lee, S. H., & Meyers, S. P. (2002). Antibacterial activity of chitosans and chitosan oligomers with different molecular weights. *International Journal of Food Microbiology, 74*(1–2), 65–72.

Notley, S. M., Eriksson, M., Wågberg, L., Beck, S., & Gray, D. G. (2006). Surface forces measurements of spin-coated cellulose thin films with different crystallinity. *Langmuir, 22*, 3154–3160.

Radtchenko, I. L., Papastavrou, G., & Borkovec, M. (2005). Direct force measurements between cellulose surfaces colloidal silica particles. *Biomacromolecules, 6*, 3057–3066.

Ramos, L. A., Assaf, J. M., El Seoud, O. A., & Frollini, E. (2005). Influence of the supramolecular structure and physicochemical properties of cellulose on its dissolution in a lithium chloride/N,N-dimethylacetamide solvent system. *Biomacromolecules, 6*, 2638–2647.

Rosca, C., Popa, M. I., Lisa, G., & Chitanu, G. C. (2005). Interaction of chitosan with natural or synthetic anionic polyelectrolytes. 1. The chitosan-carboxymethylcellulose complex. *Carbohydrate Polymers, 62*, 35–41.

Sczech, R., & Riegler, H. (2006). Molecularly smooth cellulose surfaces for adhesion studies. *Journal of Colloid and Interface Science, 301*, 376–385.

Shen, G., Anand, M. F. G., & Levicky, R. (2004). X-ray photoelectron spectroscopy and infrared spectroscopy study of maleimide-activated supports for immobilization of oligodeoxyribonucleotides. *Nucleic Acids Research, 32*(20), 5973–5980.

Silverstein, R. M., Bassler, G. C., & Morril, T. C. (1994). *Identificação espectrométrica de compostos orgânicos*. Rio de Janeiro: Guanabara Dois.

Tammelin, T., Saarinen, T., Sterberg, M. O., & Laine, J. (2006). Preparation of Langmuir/Blodgett-cellulose surfaces by using horizontal dipping procedure. Application for polyelectrolyte adsorption studies performed with QCM-D. *Cellulose, 13*, 519–535.

Wada, W. M., Nishiyama, Y., & Langan, P. (2006). X-ray structure of ammonia-cellulose I: New insights into the conversion of cellulose I to cellulose IIII. *Macromolecules, 39*, 2947–2952.

Wang, N., Chen, Y., & Kim, J. (2007). Electroactive paper actuator made with chitosan-cellulose films: Effect of acetic acid. *Macromolecular Materials and Engineering, 292*, 748–753.

Yan, L., Wang, Y., & Chen, J. (2008). Fabrication of a model cellulose surface from straw with an aqueous sodium hydroxide/thiourea solution. *Journal of Applied Polymer Science, 110*, 1330–1335.

Yokota, S., Kitaoka, T., & Wariishi, H. (2007). Surface morphology of cellulose films prepared by spin coating on silicon oxide substrates pretreated with cationic polyelectrolyte. *Applied Surface Science, 253*, 4208–4214.

Zucolotto, V., Ferreira, M., Cordeiro, M. R., Constantino, C. J. L., Balogh, D. T., Zanatta, A. R., et al. (2003). Unusual interactions binding iron tetrasulfonated phthalocyanine and poly(allylamine hydrochloride) in layer-by-layer films. *Journal of Physical Chemistry B, 107*, 3733–3737.